CHEMISTRY OF MATERIALS
Article

Chem. Mater. **2010,** *22,* 4619–4624 4619
DOI:10.1021/cm101352p

Morphological Evolution of PbSe Crystals via the CVD Route

Kibriya Ahmad, Mohammad Afzaal,[†] Paul O'Brien,*[,†] Guoxiong Hua,[‡] and J. Derek Woollins[‡]

[†]*School of Chemistry and School of Materials, The University of Manchester, Oxford Road, Manchester, M13 9PL, United Kingdom, and* [‡]*School of Chemistry, University of St. Andrews, Fife, KY16 9ST, Scotland*

Received March 2, 2010. Revised Manuscript Received July 5, 2010

The growth of highly faceted PbSe microcrystals from the aerosol-assisted chemical vapor deposition (CVD) of novel lead phosphonodiselenoato compounds $(Pb[Ph(RO)PSe_2]_2$, where R is a methyl group (Me) (**1**) or an ethyl group (Et) (**2**)) is reported. This is the first such example of growth using a CVD technique. As-deposited materials are analyzed by X-ray diffraction (XRD), scanning electron microscopy coupled with energy-dispersive X-ray analysis (SEM/EDAX), transmission electron microscopy (TEM), high-resolution transmission electron microscopy (HRTEM), and Raman spectroscopy. During the deposition studies, it has been found that the resulting morphologies are strongly dependent on the growth temperature, as a result of kinetics.

Introduction

Lead chalcogenides are extremely important in both basic scientific studies and technological applications.[1−5] Lead selenide (PbSe) is a leading material, because of its small band gap of (0.27 eV) and large bulk exciton Bohr radius (46 nm), which results in strong confinement of the electron−hole pair and large optical nonlinearity.[6] From a technological perspective, PbSe is a promising material in many applications, including laser materials,[7] thermoelectric devices,[8,9] near-infrared (near-IR) luminescence,[10] and IR detectors.[11] The recently discovered phenomenon of the multiple exciton generation (MEG) effect in PbE (where E = S, Se, or Te) materials could lead to an entirely new paradigm for high-efficiency and low-cost solar cell technology.[12−14]

The deposition of PbSe thin films have been reported by various methods, including molecular beam epitaxy,[15] electrodeposition,[16] pulse laser deposition,[17] and chemical bath deposition.[18] Reports on the growth of PbSe thin films by chemical vapor deposition (CVD) techniques are scarce.[19,20] An earlier report on the thermal decomposition[19] of $[Pb((SeP^iPr)_2N)_2]$, which is a precursor sufficiently volatile for low-pressure CVD, resulted in globular PbSe films. Later, hyperbranched structures of PbS and PbSe were reported by CVD from $PbCl_2$ and S/Se under hydrogen flow.[20] The formation of PbSe in nanocrystalline form has been demonstrated by several methods: decomposition of a single molecular precursor,[21] polymer-assisted solvothermal method,[22] soft templated routes,[18,23] electrodeposition,[24] and so on. Herein, we report the aerosol-assisted chemical vapor deposition (AACVD) from lead phosphonodiselenoato compounds $(Pb[Ph(RO)PSe_2]_2$, where R is a methyl group (Me) (**1**) or an ethyl group (Et) (**2**)) to give PbSe films/crystals on glass and $Si/SiO_2(100)$ substrates, which are new precursors for this material. Deposition on $Si/SiO_2(100)$ substrates leads to highly faceted PbSe micrometer-sized crystals with morphology strongly influenced by growth temperatures.

*Author to whom correspondence should be addressed. E-mail: paul.obrien@manchester.ac.uk.

(1) Alivisatos, A. P. *Science* **1996**, *271*, 933.
(2) Wang, Y.; Herron, N. *J. Phys. Chem.* **1991**, *95*, 525.
(3) Calvert, P. *Nature* **1999**, *399*, 210.
(4) Hu, J.; Odom, T. W.; Lieber, C. M. *Acc. Chem. Res.* **1999**, *32*, 435.
(5) Cheng, C. W.; Xu, G. Y.; Zhang, H. Q.; Luo, Y. *J. Nanosci. Nanotechnol.* **2007**, *7*, 4439.
(6) Lifshitz, E.; Bashouti, M.; Kloper, V.; Kigel, A.; Eisen, M. S.; Berger, S. *Nano Lett.* **2003**, *3*, 857.
(7) Cui, D. H.; Xu, J.; Zhu, T.; Paradee, G.; Ashok, S.; Gerhold, M. *Appl. Phys. Lett.* **2006**, *88*, 183111.
(8) Harman, T. C.; Taylor, P. J.; Walsh, M. P.; LaForge, B. E. *Science* **2002**, *297*, 2229.
(9) Murray, C. B.; Sun, S.; Gaschler, W.; Doyle, H.; Betley, T. A.; Kagan, C. R. *IBM J. Res. Dev.* **2001**, *45*, 47.
(10) Schaller, R. D.; Petruska, M. A. P.; Klimov, V. I. *J. Phys. Chem. B* **2003**, *107*, 13765.
(11) Qi, D.; Fischbein, M.; Drndic, M.; Selmic, S. *Appl. Phys. Lett.* **2005**, *86*, 093103.
(12) Elingson, R. J.; Beard, M. C.; Johnson, J. C.; Shabaev, A.; Efros, A. L. *Nano Lett.* **2005**, *5*, 865.
(13) Allan, G.; Delerue, C. *Phys. Rev.* **2006**, *B73*, 205423.
(14) Nozik, A. J. *Chem. Phys. Lett.* **2008**, *457*, 3.
(15) Zhao, F.; Mukherjee, S.; Ma, J.; Li, D.; Elizondo, S. L.; Shi, Z. *Appl. Phys. Lett.* **2008**, *92*, 211110.
(16) Shah, A. A.; Holze, R. *Electrochim. Acta* **2008**, *53*, 4642.
(17) Evstratov, I. Y.; Kalaev, V. V.; Zhmakin, A. I.; Makarov, Y. N.; Abramov, A. G.; Ivanov, N. G.; Smirnov, E. M.; Dornberger, E.; Virbulis, J.; Tomzig, E.; Ammon, W. V. *J. Cryst. Growth* **2001**, *230*, 22.
(18) Gorer, S.; Albu-Yaron, A.; Hodes, G. *Chem. Mater.* **1995**, *7*, 1243.
(19) Afzaal, M.; Ellwood, K.; Pickett, N. L.; O'Brien, P.; Raftery, J.; Waters, J. *J. Mater. Chem.* **2004**, *14*, 1310.
(20) Bierman, M. J.; Lau, Y. K. A.; Jin, S. *Nano Lett.* **2007**, *7*, 2907.
(21) Trindade, T.; Monteiro, O. C.; O'Brien, P.; Motevalli, M. *Polyhedron* **1999**, *18*, 1171.
(22) Cheng, C.; Xu, G.; Zhang, H. *J. Cryst. Growth* **2009**, *311*, 1285.
(23) Liu, Y. F.; Cao, J. B.; Zeng, J. H.; Li, C.; Qian, Y. T.; Zhang, S. Y. *Eur. J. Inorg. Chem.* **2003**, 644.
(24) Das, D. V.; Bhat, K. S. *J. Mater. Sci.* **1990**, *25*, 169.

Published on Web 07/22/2010

Scheme 1. Synthesis of Compounds 1 and 2

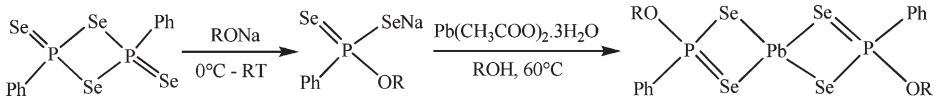

Experimental Section

Both the complexes $Pb[Ph(RO)PSe_2]_2$ (where R = Me (**1**) or Et (**2**)) were prepared using the reported method.[25] Thermogravimetric analysis (TGA) was conducted using a Seiko Model SSC/S200 system at a heating rate of 10 °C min^{-1} under N_2 between 25 °C and 600 °C. X-ray diffraction (XRD) studies were carried out using Cu Kα radiation on a Bruker AXS D8 advance diffractometer. The samples were mounted flat and scanned over a 2θ range of 20° to 80°, in steps of 0.05° with a count time of 5.5 s. The films were carbon-coated, using an Edwards Model e306A coating system before performing the image analyses. Scanning electron microscopy (SEM) analyses were performed using a Philips Model XL 30FEG instrument, whereas energy-dispersive X-ray analysis (EDAX) was carried out using a DX4 instrument. Transmission electron microscopy (TEM) analyses were conducted using the Tecnai F30 instrument operating at up to 300 kV, and a Ramanscope System 2000 spectrophotometer in the range of 135−500 cm^{-1} with an excitation wavelength of 632.8 nm was utilized for Raman spectroscopy studies.

The deposition of films from both compounds was carried out on glass and $Si/SiO_2(100)$ substrates. The glass microscope slides were kept in dilute nitric acid overnight and then rinsed with deionized water. The $Si/SiO_2(100)$ substrates were thoroughly cleaned using a literature procedure.[26] In a typical deposition, 0.1 g of the precursor was dissolved in 10 mL toluene in a round-bottom flask. The argon flow rate, which was controlled by a platon flow gauge, was kept constant at 160 sccm throughout the CVD studies. Three glass or $Si/SiO_2(100)$ substrates (ca. 1 cm × 1 cm) were placed inside the reactor tube and then heated at the desired temperature for 10 min before carrying out the deposition. The aerosol of the precursor solution was formed by keeping the round-bottomed flask in a water bath above the piezoelectric modulator of a Pifco ultrasonic humidifier (Model 1077). The aerosol droplets of the precursor thus generated were transferred into the hot wall zone of the reactor by the carrier gas. The reactor was placed in a Carbolite furnace.

Results and Discussion

Both complexes **1** and **2** were prepared by the reaction of lead acetate with two equivalents of sodium phosphonodiselenoate in high yield; the latter was derived from 2,4-bis(phenyl)-1,3-diselenadiphosphetane-2,4-diselenide $[PhP(Se)(\mu\text{-}Se)]_2$ (Woollins Reagent) with the corresponding sodium alkoxide (see Scheme 1).[25] The compounds were relatively air-stable at room temperature and had good solubility in high-boiling-point solvents.

The physical behavior determined by TGA (under N_2, 10 °C/min) indicated that the decomposition occurs in two unresolved steps in the temperature ranges of 195−391 °C for **1** and 169−405 °C for **2** (see Figures S1 and S2 in the Supporting Information). The residual mass for compound **1** can be tentatively assigned to bulk PbSe (wt % left 40%, calcd 36%). However, in the case of compound **2**, a larger residue is observed (wt % left 44%, calcd 35%), probably as a result of some side products of decomposition, such as selenium contamination.

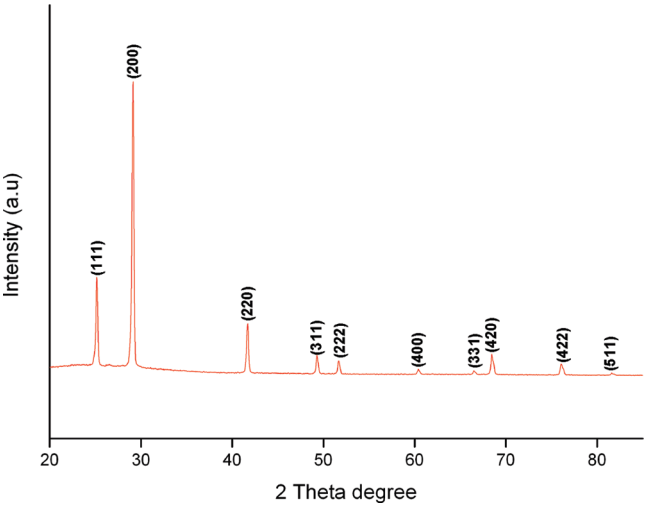

Figure 1. Typical XRD pattern of PbSe film on glass at 400 °C from compound **1**.

Because of the poor volatility of the compounds, deposition experiments were conducted in a AACVD kit at 300−500 °C for 1 h. During the initial CVD runs, it was determined that a temperature of 300 °C was too low to initiate deposition. At > 400 °C, dusty metallic films were formed and were determined to be nonadherent, as they could be easily removed from the surface. Prior to each deposition run, substrates were heated under argon at growth temperatures for 30 min to eliminate the formation of any residual oxygen-containing species.

The XRD patterns of as-deposited materials on glass confirmed the formation of pure PbSe films at all deposition temperatures (International Centre for Diffraction Data (ICDD) File Card No. 04-04-4328). A typical XRD pattern for a cubic PbSe film (deposited at 400 °C from compound **1**), which has a preferred orientation along the (200) plane with a full width at half-maximum (fwhm) of 0.2°, is shown in Figure 1. The calculated unit-cell parameters and fwhm of all the films are presented in Table 1 and are in good agreement with the literature value. Scanning electron microscopy (SEM) studies were carried out to analyze the morphology of deposited materials. Deposition experiments conducted on glass using compound **1** yielded a variety of different products, depending on the substrate temperature (see Figure 2). The morphology of the material deposited at 300 °C consisted of rows of interlocked plates surrounded by globular material. However, at 400 °C, micrometer-sized truncated octahedrons embedded in the globular film were clearly visible. At the highest temperature (500 °C), only globular

(25) Gray, I. P.; Slawin, A. M. Z.; Woolins, J. D. *Dalton Trans.* **2005**, 2188.
(26) http://www.virginiasemi.com/pdf/siliconetchingandcleaning.pdf (accessed May 2010).

Table 1. Calculated Unit-Cell Parameters for All the Deposited Materials[a]

temperature (°C)	compound	substrate	lattice constant (Å)
300	**1**	glass	6.125
400	**1**	glass	6.126
500	**1**	glass	6.126
300	**2**	glass	6.120
400	**2**	glass	6.127
500	**2**	glass	6.123
300	**1**	Si/SiO_2	6.126
400	**1**	Si/SiO_2	6.126
500	**1**	Si/SiO_2	6.125
300	**2**	Si/SiO_2	6.127
400	**2**	Si/SiO_2	6.126
500	**2**	Si/SiO_2	6.125

[a] The literature value for cubic PbSe (ICDD No. 04-04-4328) is $a = 6.128$ Å.

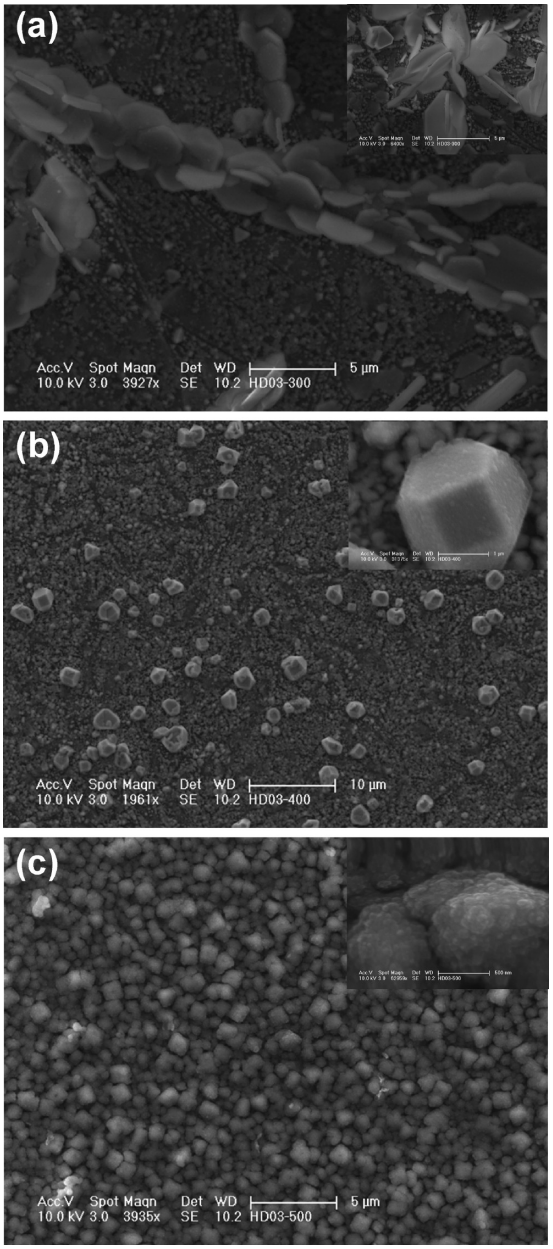

Figure 2. SEM images of PbSe films deposited on glass at (a) 300 °C, (b) 400 °C, and (c) 500 °C on glass from compound **1**. Insets are the corresponding high-resolution scanning electron microscopy (HR-SEM) images.

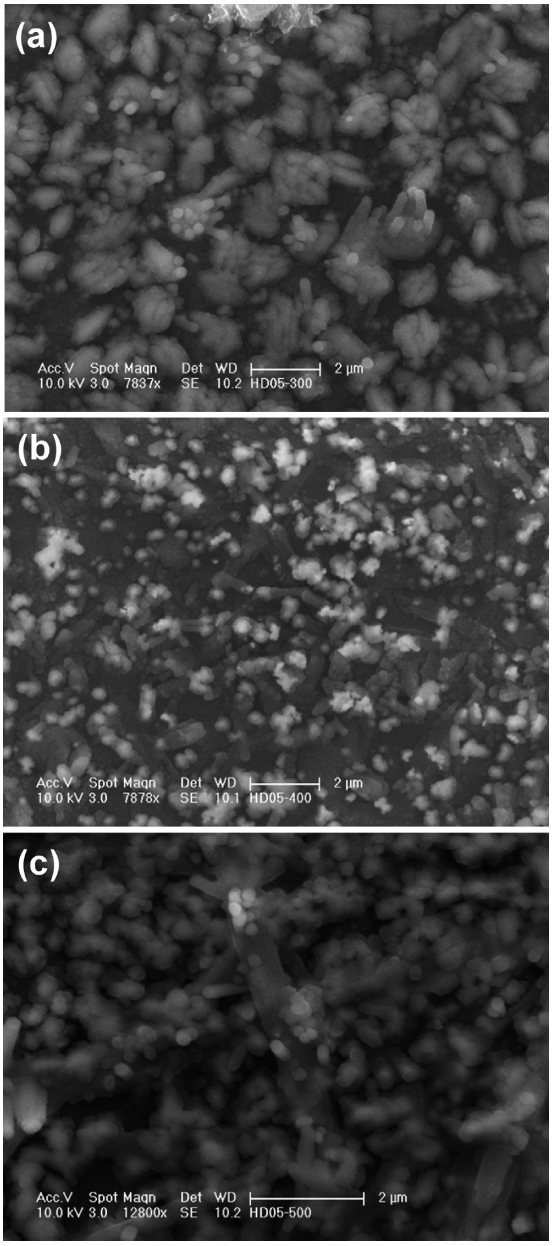

Figure 3. SEM images of PbSe films deposited on glass at (a) 300 °C, (b) 400 °C, and (c) 500 °C on glass from compound **2**.

material was observed. CVD growth runs conducted using compound **2** on glass produced globular rod-type material in all cases (see Figure 3). Quantitative EDAX analysis of all resulting materials showed a Pb:Se ratio of 1:1 (within the errors of the method).

Further AACVD experiments were conducted on $Si/SiO_2(100)$ substrates using the same conditions as those for the glass substrates. The XRD measurements confirmed the formation of cubic PbSe (ICDD No. 04-04-4328) from both compounds. The XRD spectra that resulted from compound **1** at 300−500 °C are shown in Figure 4. The calculated lattice constants given in Table 1 are in good agreement with the literature value ($a = 6.128$ Å). As the growth temperature increases, a correlation between an increase in intensity of the (200) peak and a decrease in the (111) peak emerges. A decrease in the relative intensity of (111) reflection indicates that growth along the (111)

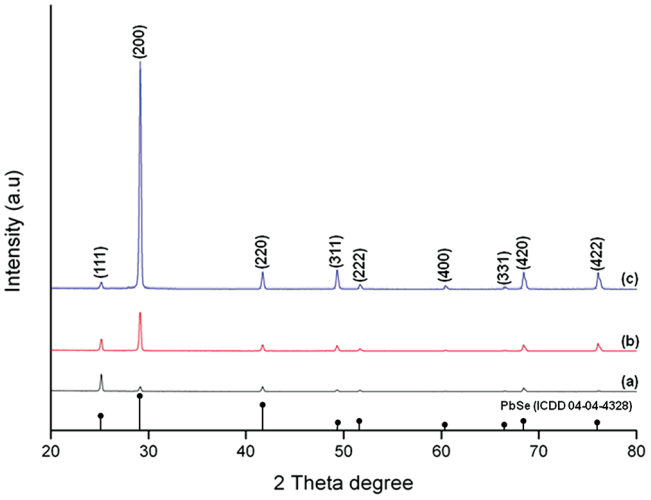

Figure 4. XRD of PbSe films on Si/SiO_2 at (a) 300 °C, (b) 400 °C, and (c) 500 °C from compound **1**.

direction is taking place, thus promoting the formation of (100) facets. At lower growth temperature, the growth along the (100) direction increases, resulting in the elimination of the (100) facets and promoting the formation of (111) facets.

The SEM images shown in Figure 5 for compound **1** deposited on Si/SiO_2 indicated two types of PbSe crystals: micrometer-sized octahedrons at 300 and 400 °C and cubes at 500 °C. It is also evident that the density of the particles increases as the growth temperature increases. The crystallites were scattered on the Si/SiO_2 surface, which resulted in a discontinuous film. This may be a result of poor wetting between the PbSe crystallites and silicon substrate.[27] The crystal morphology of PbSe crystals is dependent on the relative rates of growth in the (100) and (111) direction. The formation of octahedra suggests that the PbSe crystal growth is faster in the low-energy (100) direction.[28] The driving force behind the transformation from octahedrons to cubes may lie in the fact that the growth rate in the (111) direction is greater than that in the (100) direction.[29−31] The highest growth temperature (500 °C) seems to shift crystal growth into a thermodynamic regime. These observations suggest that the growth of symmetric PbSe crystals is very sensitive to the deployed kinetic conditions in the CVD system. Unlike previous studies, no stabilizers (e.g., polyacrylamide[22] or poly(vinylpyrrolidone),[32] or any other amines[33]) were used to manipulate the surface energy of the different facets, which might result in the evolution of a different morphology.

To gain further insight into the mechanism, growth runs were conducted for 5 and 10 min at 400 °C using compound **1** on $Si/SiO_2(100)$ substrates (see Figure 6). After 5 min, small PbSe crystals that are truncated octahedron

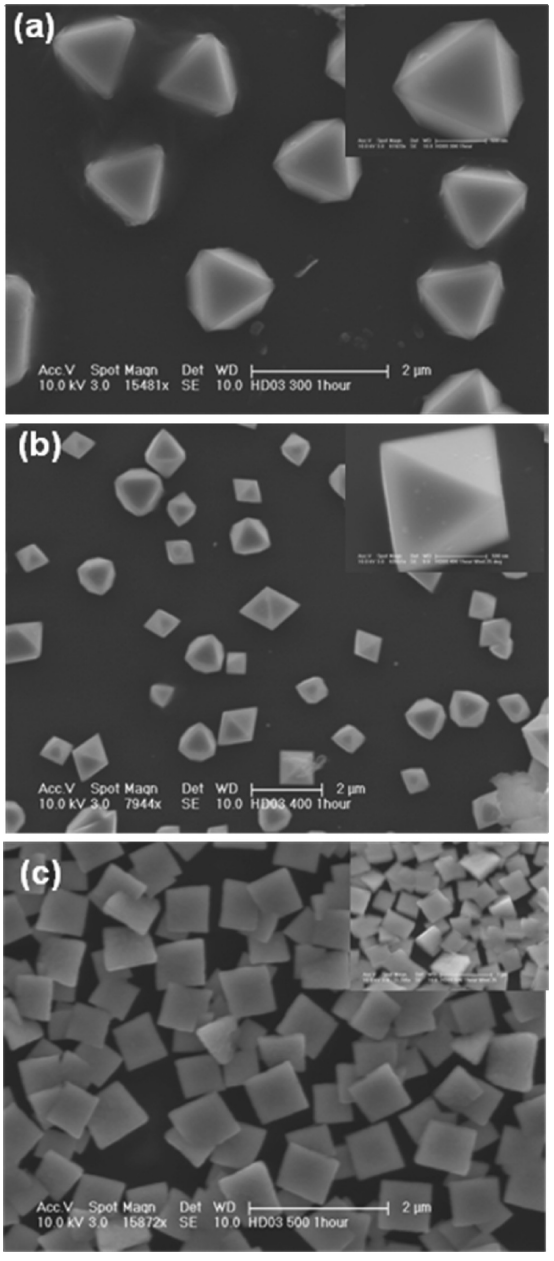

Figure 5. SEM images of PbSe crystals deposited on Si/SiO_2 at (a) 300 °C, (b) 400 °C, and (c) 500 °C from compound **1**. Insets are the corresponding HR-SEM images.

through their (111) facets clearly have a tendency to aggregate. The promotion of surface domains on neighboring particles, to match up by sharing their (111) face, leads to an increase in lower-index planes and satisfies geometric criterion and dipole interactions of low energy.[34−40] After 10 min, truncated octahedrons are

(27) Shandalov, M.; Golan, Y. *Eur. Phys. J. Appl. Phys.* **2005**, *31*, 27.
(28) Houtepen, A. J.; Koole, R.; Vanmaekelbergh, D.; Meeldijk, J.; Hickey, S. G. *J. Am. Chem. Soc.* **2006**, *128*, 6792.
(29) Petroski, J. M.; Wang, Z. L.; Green, T. C.; El-Sayed, M. A. *J. Phys. Chem. B* **1998**, *102*, 3316.
(30) Dowty, E. *Am. Mineral.* **1976**, *61*, 448.
(31) Fan, D. B.; Thomas, J. P.; O'Brien, P. *J. Am. Chem. Soc.* **2008**, *130*, 33.
(32) Peng, Z.; Jiang, Y.; Song, Y.; Wang, C.; Zhang, H. *Chem. Mater.* **2008**, *20*, 3153.
(33) Tang, Z.; Kotov, N. A.; Giersig, M. *Science* **2002**, *297*, 237.
(34) Pacholski, C.; Kornowski, A.; Weller, H. *Angew. Chem., Int. Ed.* **2002**, *41*, 1188.
(35) Korgel, B. A.; Fitzmaurice, D. *Adv. Mater.* **1998**, *10*, 661.
(36) Lu, W.; Gao, P.; Jian, W. B.; Wang, Z. L.; Fang, J. *J. Am. Chem. Soc.* **2004**, *126*, 14816.
(37) Tang, Z. Y.; Zhang, Z. L.; Wang, Y.; Glotzer, S. C.; Kotov, N. A. *Science* **2006**, *314*, 274.
(38) Harfenist, S. A.; Wang, Z. L.; Alvarez, M. M.; Vezmar, I.; Whetten, R. L *Adv. Mater.* **1997**, *9*, 817.
(39) Wang, Z. L. *Adv. Mater.* **1998**, *10*, 13.
(40) Cho, K. S.; Talapin, D. V.; Gaschler, W.; Murray, C. B. *J. Am. Chem. Soc.* **2005**, *127*, 7140.

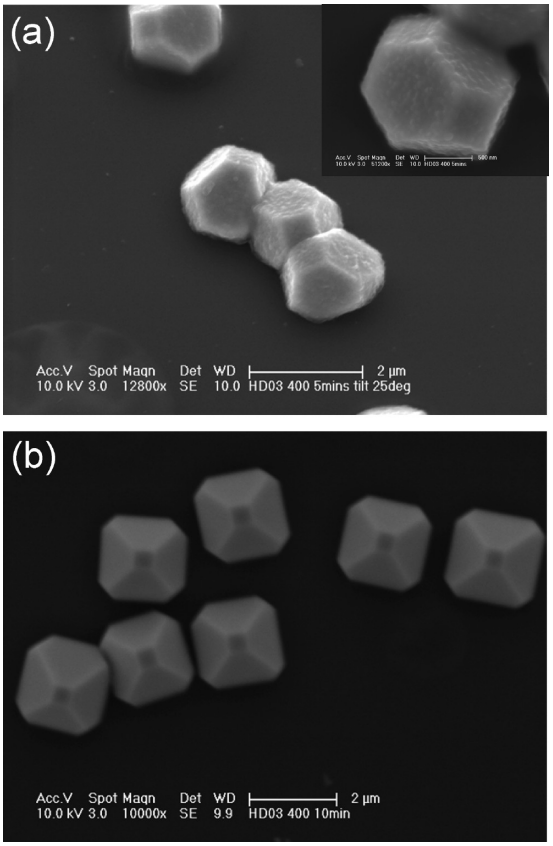

Figure 6. SEM images of PbSe crystals deposited after (a) 5 min and (b) 10 min on Si/SiO_2 from compound **1**. Inset in panel (a) shows a HR-SEM image.

generally observed by exposing their (100) facets (see Figure 6b).

The resulting SEM images of deposited material from compound **2** on $Si/SiO_2(100)$ are shown in Figure 7. At 300 °C, a mixture of poorly defined octahedrons and rods is evident. However, at 400 and 500 °C, octahedrons and 0D truncated cubic (tetradecahedron)-shaped PbSe crystals are deposited, respectively. The evolution of truncated cubes involves the cuboctahedral seed growing along the (111) plane at a higher growth rate than that of the (100) plane. It is predicted that different growth products from compounds **1** and **2** under similar deposition conditions could be a result of different thermal behaviors and provide different decomposition pathways for the nucleation of the crystals. The stoichiometry of all grown crystals was confirmed by EDAX analysis (1:1), and no impurities such as phosphorus or nitrogen were detected (see Figure S3 in the Supporting Information).

The TEM and HRTEM images of octahedron deposited at 400 °C from compound **2** on $Si/SiO_2(100)$ are shown in Figure 8. The HRTEM image shows a lattice spacing of 0.359 nm, which is consistent with the (111) plane of cubic PbSe (ICDD No. 04-04-4328; lit. value = 0.353 nm). Within the same image, the lattice fringes indexed to the (110) plane can also be found (calc. 0.218 nm; lit. 0.217 nm). The SAED pattern of te same image shows clear diffraction spots, indicating single crystallinity of the octahedrons. Note that six almost symmetrical elongated spots appear

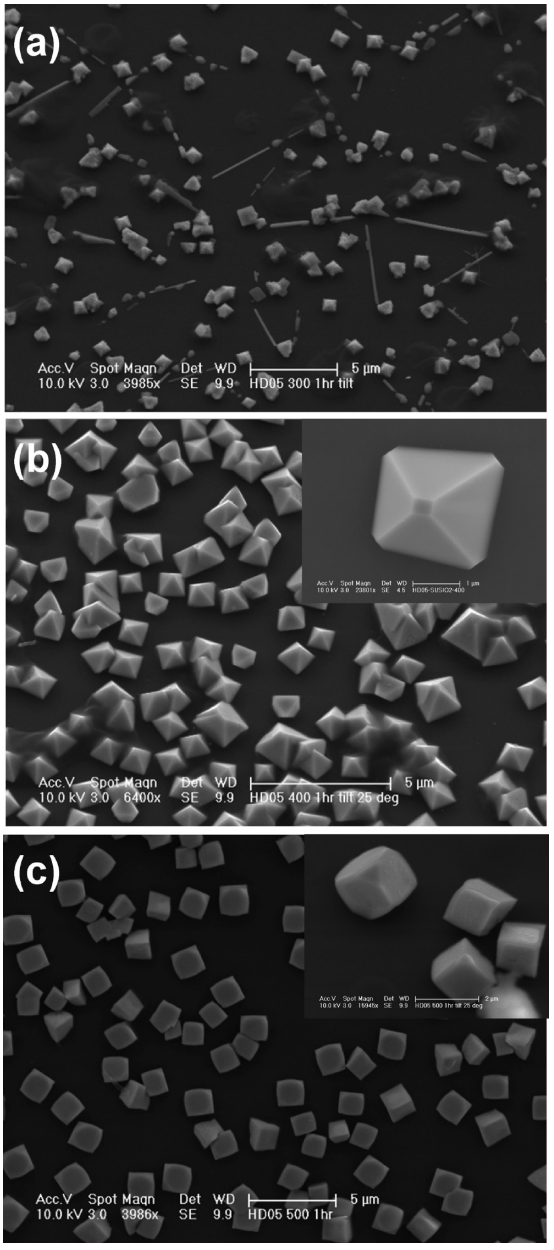

Figure 7. SEM images of PbSe crystals deposited at (a) 300 °C, (b) 400 °C, and (c) 500 °C on Si/SiO_2 from compound **2**. Insets are the corresponding HR-SEM images.

in the ring of the (220), indicating the preferentially orientated octahedrons at the interfaces with the (111) zone nearly parallel to the incident electron beam.

To compliment XRD results, Raman spectra of the PbSe cubes grown from compound **1** at 500 °C on $Si/SiO_2(100)$ were obtained using a helium−neon (He−Ne) laser operating at 632.8 nm at room temperature, which led to Raman-active vibrational modes. The signal integration time was 30 s. A typical Raman spectrum of the PbSe cubes with 50 mW laser power is shown in Figure 9. The first-order longitudinal optical phonons at the Γ-point of the Brillouin zone (LO) at 138 cm^{-1} is in a similar position to the earlier report.[41] The weaker structure at

(41) Upadhyaya, K. S.; Yadav, M.; Upadhyaya, G. K. *Phys. Status Solidi B* **2002**, *229*, 1129.

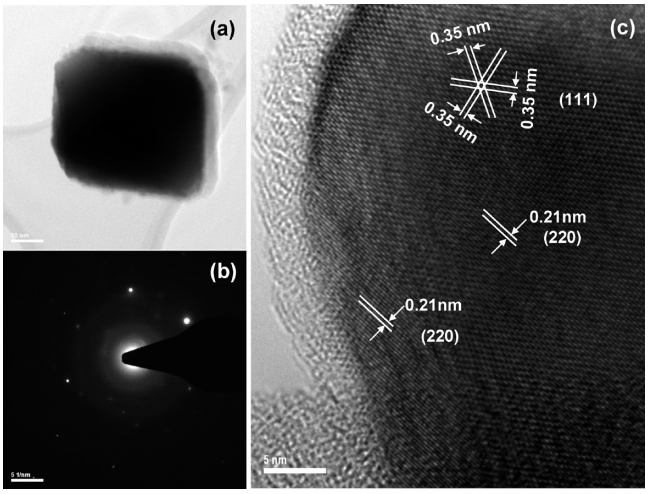

Figure 8. (a) TEM and (c) HRTEM image of octahedron from compound **2** on Si/SiO_2 at 400 °C. (b) is the corresponding SAED pattern.

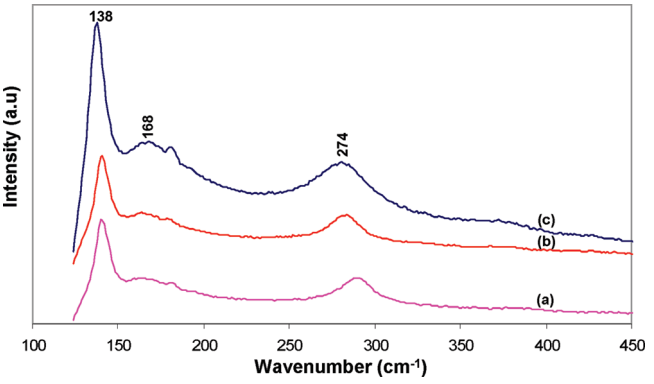

Figure 9. Raman spectra of PbSe crystals deposited using compound **1** on $Si/SiO_2(100)$ with different laser powers of 50 mW: (a) 25%, (b) 50%, and (c) 100%.

168 cm^{-1} is assigned to 2LO(X), although several wave numbers shift from the theoretical value.[41] The broad peak at 274 cm^{-1} is associated with two phonon scattering (2LO). Longitudinal optical phonons are responsible for the Raman shifts in crystalline semiconductors. In contrast, surface phonons and transverse optical phonons are not observable, because of the low intensities and symmetry restrictions.[42] Unlike previous studies, no evidence of photodegradation of PbSe crystals was detected as a result of an increase in the laser power, which might be due to the absence of any organic substituents. However, it is apparent that the Raman shifts are slightly blue-shifted as the laser power is increased incrementally. It is well-known that PbSe material has very low thermal conductivity[43] and any increase in the local temperature that is due to the use of high power on the focused laser spot could result in Raman shift.

Conclusion

The control over crystal growth has been displayed in synthesizing submicrometer cubes, truncated octahedrons, and octahedron via a single source route. The shapes of the as-obtained PbSe crystals can be controlled by choosing different ligands, and the ratio of (111) to (100) facets of the nanocrystal that are exposed can also be manipulated. It has also been shown that variation in growth temperatures can have a profound effect on the growth of PbSe crystals. This report provides a simple and efficient way to control the surface properties of highly faceted PbSe crystals.

Acknowledgment. The authors are grateful to the University of Manchester and the Engineering and Physical Science Research Council (EPSRC, UK) for financial support.

Supporting Information Available: TGA of $Pb[Ph(MeO)PSe_2]_2$ (**1**) (Figure S1) and $Pb[Ph(EtO)PSe_2]_2$ (**2**) (Figure S2), as well as a typical EDAX spectrum of PbSe truncated cubes formed at 500 °C on Si/SiO_2 (100) from **2** (Figure S3). (PDF) This material is available free of charge via the Internet at http://pubs.acs.org.

(42) Wang, N.; Cao, X.; Guo, L.; Yang, S.; Wu, Z. *ACS Nano* **2008**, *2*, 2.

(43) Li, K. W.; Meng, X.; Liang, X.; Wang, H.; Yan, H. *J Solid-State Electrochem.* **2006**, *10*, 48.